Optical Materials: X 14 (2022) 100154

Contents lists available at ScienceDirect

Optical Materials: X

journal homepage: www.journals.elsevier.com/optical-materials-x

Characterization of pasteurized milk in the near infrared range for construction of tissue-mimicking optical phantoms

Wesam Bachir [a,b,*], Rewa khir [a]

[a] Biomedical Photonics Laboratory, Higher Institute for Laser Research and Applications, Damascus University, Damascus, Syria
[b] Faculty of Informatics Engineering, Al-Sham Private University, Damascus, Syria

ARTICLE INFO

Keywords:
Pasteurized milk
NIR spectroscopy
Diffuse reflectance
Collimated transmission
Optical phantoms

ABSTRACT

Optical phantoms have been indispensable tools for validating the performance of biomedical optical devices. Low-cost and readily available materials are gaining great interest for the construction of biomedical optical phantoms. The main objective of this work is to investigate the feasibility of using commercial pasteurized milk as a scattering component of optical phantoms. To that end, milk samples with varying concentrations were prepared. Transmittance and diffuse reflectance spectroscopy at 690 and 830 nm were measured for milk samples. Then, the optical properties of pasteurized milk were determined. The results demonstrate the suitability of using pasteurized milk as a potential scattering element for building tissue-simulating optical phantoms in the NIR range of wavelength. Low fat pasteurized milk samples outperformed full-fat milk samples resulting in lower uncertainty levels in estimating scattering coefficient at 690 and 830 nm. The effect of batch-to-batch variation on scattering coefficient evaluation is investigated and discussed. The preliminary findings of this work provide a base for the rapid preparation of scattering-dependent optical phantoms needed for the validation and calibration of biomedical optical instrumentation.

1. Introduction

Recent advancement in biophotonics applications in medicine requires the use of optical phantoms for validation of measurements, the calibration of newly developed biomedical optical instrumentation, and evaluation of the performance of existing optical devices prior to clinical measurements [1]. Most of the materials used for making such phantoms can be expensive. In addition, the fabrication process for some optical phantoms can be challenging and time-consuming [2]. Thus, there has been a growing interest by researchers in the use of low-cost, readily available, and easy-to-construct tissue-like optical phantoms [3,4].

Essentially, the construction of optical phantoms requires a combination of scattering and absorbing materials. They are designed with optical properties that match the optical properties of biological tissue of interest over a specific range of wavelengths. Different materials have been used as scattering elements. Recently, Tomm et al. [5] proposed a method for characterizing the optical properties of silicone soluble color pastes as a promising step towards the production of long-term stable optical phantoms that mimic biological tissue with specific oxygenation levels.

As for scattering materials, Lipid-based materials, notably Intralipid have been extensively used by researchers for building optical phantoms to represent the scattering component [6–8]. However, despite its wide use in constructing optical phantoms, Intralipid can be quite expensive, particularly in low-resource settings. Alternatively, milk has been used as a viable substitute to simulate scattering in tissue. Although milk can be stable only for a few hours and features limited low reproducibility between samples [1], it is readily available and exhibits real compatibility with biological tissue with an index of refraction around 1.45.

Moreover, several recent previous studies have focused on investigating the quality of raw milk content of protein and fat [9]. For that, different optical methods were used such as oblique incidence reflectometry [10], spatially resolved diffuse reflectance spectroscopy [11], and photon time-of-flight spectroscopy [12].

Aernouts et al. [13] measured the optical properties of raw milk to monitor the quality of dairy milk. They used a double integrating sphere and unscattered transmittance measurements to determine the bulk optical properties of the milk samples in the visible and near-infrared range of wavelengths, as this technique was considered the gold standard method for optical properties measurement of thin samples of turbid media.

Moreover, Jain and Sarma [14] Introduced a digital imaging-based

* Corresponding author. Biomedical Photonics Laboratory, Higher Institute for Laser Research and Applications, Damascus University, Damascus, Syria.
E-mail address: w.b.foit@aspu.edu.sy (W. Bachir).

https://doi.org/10.1016/j.omx.2022.100154
Received 11 January 2022; Received in revised form 22 April 2022; Accepted 22 April 2022
Available online 6 May 2022

method for online spectrophotometric analysis of raw milk. They used multiple LEDs of different emission spectra as discrete light sources and a digital CMOS camera as a detector. The extinction characteristic of samples can be derived from captured images. However, their method requires the use of a camera and further image analysis of the collected image. This can be impractical in limited resources settings thus compact and readily available materials and methods are needed.

Optical spectroscopy, imaging, and therapy tissue phantoms must have the scattering and absorption properties that are characteristic of human tissues. The most widely used phantoms for optical imaging and spectroscopy have been the liquid type, made from milk that mimics the scattering of biological tissue of interest, especially in the near-infrared range of wavelength.

Pasteurized milk is dairy milk that is heated and cooled using a simple heating process that makes milk safe to drink before it is packaged and shipped to grocery stores. To the best of our knowledge, pasteurized milk has not been investigated as a scattering component of optical phantoms. Therefore, our goal in this paper is to present simple optical methods based on laser collimated transmission and diffuse reflectance spectroscopy to characterize the optical properties of pasteurized milk-based phantoms at two distinct wavelengths commonly used in near-infrared spectroscopy. The suitability of using pasteurized milk as a scattering material in optical phantoms is validated and discussed.

2. Materials and methods

For optical characterization of the pasteurized milk, optical phantoms were constructed then optical measurements were implemented to determine the optical properties mainly attenuation and scattering coefficients of the pasteurized milk samples. The determination of attenuation and scattering coefficients was achieved using two optical setups, the first setup, called collimated transmission spectroscopy, was used to estimate the attenuation coefficient of the pasteurized milk followed by a second setup called diffuse reflectance spectroscopy that enabled the determination of the scattering coefficient of pasteurized milk. Since pasteurized milk samples are turbid media exhibiting both absorption and scattering properties, estimating the scattering coefficient using the second method requires prior knowledge of the attenuation coefficient that resulted from the transmission measurements. Sample preparation and optical methodology used in this work are described in the following subsections.

2.1. Optical phantoms

Optical phantoms in this study were made of pasteurized milk. Commercially packaged pasteurized milk (Hawa AlSham Inc. Syria) was used in this work. Two types of pasteurized milk were used in this work. Low fat (0g/100 mL) and full fat (3g/100 mL) packaged pasteurized milk were used as a stock solution for the optical measurements. The samples were diluted in distilled water and prepared in ten different concentrations ranging from 0.01% to 0.1% for pasteurized milk. Samples preparation and consequent optical measurements were made within less than 1 h. Each sample was kept in a plastic cuvette having a light path of 10 mm.

For highly diffusive media there are two ways to avoid the influence of multiple scattered light on the measurement, either the sample can be diluted or the thickness of the cuvette can be decreased [15]. In this study, the milk sample was diluted with water to a concentration of less than 1% (volume, milk to water), which is considered low enough to avoid the influence of multiple scattering on the measurement [16].

2.2. Fiber-optic collimated transmittance

In this work, a fiber optic-based transmittance measurement was used to quantify the attenuation coefficient of pasteurized milk-based optical phantoms.

Fig. 1a shows an overview of the optical setup used to measure the total attenuation coefficient of milk samples. For transmission measurements, pasteurized milk-based samples were inserted in a cuvette holder equipped with an in-line fibre-optic filter holder (CUV-ATT-DA, Avantes Inc., Netherlands) and an attenuator (ATT-INL-EXT, Avantes Inc., Netherlands), however, the filter holder was not used in this study.

The cuvette holder device is equipped with two collimating lenses mounted before and after the cuvette and the in-line attenuator also has two collimating lenses on either side of an adjustable iris. The collimating lenses in the in-line attenuator provide further collimation of the transmitted beam before being detected by a spectrometer. For this measurement, the iris (adjustable screw 2) was set at 100%.

The optical set-up comprises two fiber-coupled diode lasers operating at 830 and 690 nm (PDLD, USA). Each laser can be mounted inside a laser controller (LDM9LP, THORLABS Inc) as shown in Fig. 1b. The lasers were driven by a current driver (LDC210C, THORLABS Inc) and operated in continuous wave mode (CW).

A small, compact, and portable spectrometer (USB4000 FL, Ocean Optics Inc.), with optical fiber (EOS-A1221738, Ocean Optics Inc., Dunedin, Florida, USA), was used for collecting the transmittance spectra. The spectrometer was connected via USB cable to the computer for acquiring transmission spectra using Spectra Suit software (Ocean Optics Inc., 2011) for further analysis.

The total attenuation coefficient μ_t was calculated using the well-known Beer-Lambert law using the following expression [15,17].

$$I_z(\lambda) = I_o(\lambda).e^{-\mu_t(\lambda).z} \tag{1}$$

or alternatively,

$$I_z(\lambda) = I_o(\lambda).e^{-ex(\lambda).z.c} \tag{2}$$

where c is the concentration, z is the optical path length of the laser beam in the turbid medium, $I_o(\lambda)$ is the incident intensity, $ex(\lambda)$ is the extinction coefficient and $I_z(\lambda)$ is the measured transmitted intensity.

Transmittance was calculated by the following equation

$$T(\%) = I_z(\lambda)/I_o(\lambda) \tag{3}$$

where $I_o(\lambda)$ in eq. (3) is the measured transmitted intensity from a distilled water sample and $I_z(\lambda)$ is the measured transmitted intensity from the milk sample. The Absorbance A can also be related to the Transmittance using the following expression

$$A = 2 - log10(T) \tag{4}$$

Then, the calculated absorbance, extinction coefficient, and attenuation coefficient are used for calculating the scattering coefficient μ_s of pasteurized milk samples based on the diffuse reflectance measurements as described in the next section.

2.3. Diffuse reflectance spectroscopy

To measure the reduced scattering coefficient $\mu_{s'}$ of milk samples, the block diagram of the optical setup shown in Fig. 2a below was implemented in this study.

The optical set-up used for diffuse reflectance spectroscopic measurements consists of two fiber-coupled diode lasers operating at 830 and 690 nm (PDLD, USA), that can be mounted separately inside a laser controller (LDM9LP, THORLABS Inc), The lasers were driven by a current driver (LDC210C, THORLABS Inc) as shown in Fig. 2b. In this setup, the illumination fiber was positioned at a 90^0 with the help of a reflection probe holder (RPH-1, Ocean Optics, USA). Then, a portable spectrometer (USB4000 FL, Ocean Optics Inc.), with a fiber-optic probe (R600-7-VIS-125F, Ocean Optics Inc., Dunedin, Florida, USA) positioned at a 45^0 by the same reflection probe holder, was used to record the spectrum of back-reflected laser from within the phantom. Diffuse

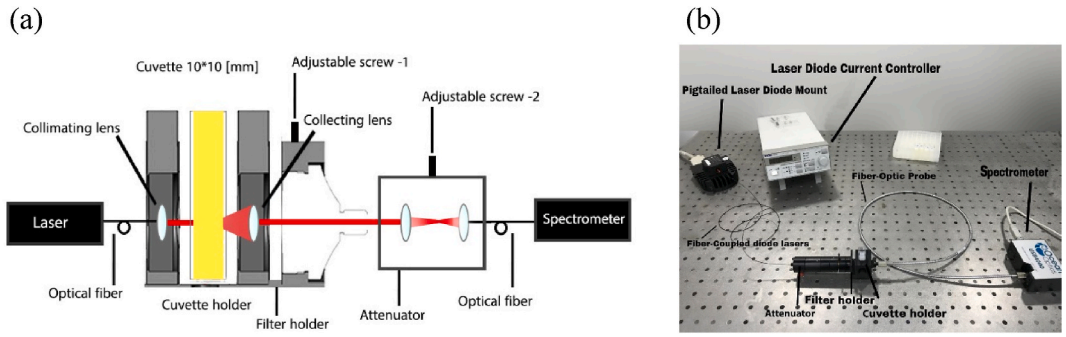

Fig. 1. (a) Schematic overview of the collimated transmission setup illustrating the milk sample in cuvette holder (b) Experimental optical setup for collimated transmission measurements.

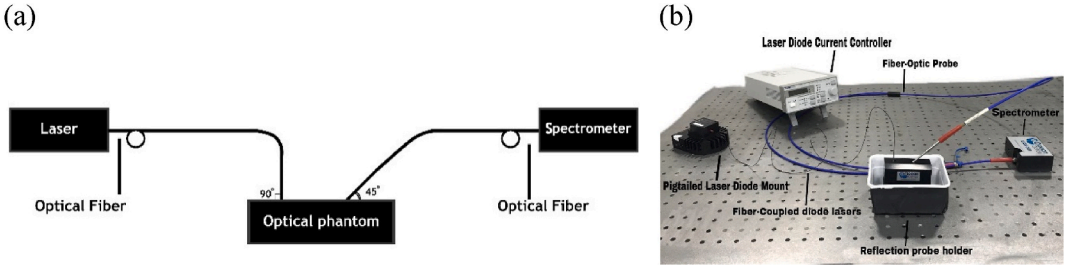

Fig. 2. (a) Schematic overview of the optical setup used for measuring diffuse reflectance, (b) Experimental diffuse reflectance measurement.

reflectance measurements with a tilted probe at 45^0 were carried out to reduce the specular reflectance in the measurements. A reflectance standard (WS-1, Ocean Optics Inc., Dunedin, Florida, USA) was used for calibrating the diffuse reflectance measurements before each session. Additionally, dark current and background measurements were taken at the same setting before each recording.

In principle, the reduced scattering coefficient $\mu_{s'}$ can be expressed as [18].

$$\mu_{s'} = \mu_s(1-g) \tag{5}$$

where g is the anisotropy factor and μ_s is the scattering coefficient, the diffuse reflectance spectroscopy spectrum of the samples was measured and can be related to reduced albedo a' by the following equation [19].

$$R_\infty = \frac{a'}{1+2k.(1-a')+(1+\frac{2K}{3}).\sqrt{3(1-a')}} \tag{6}$$

where R_∞ is the measured diffuse reflectance given by

$$R_\infty = r_{sample}/r_{standard} \tag{7}$$

where $r_{standard}$ is the diffuse reflectance of the standard calibration sample and r_{sample} is the diffuse reflectance of the milk sample, a' is the reduced albedo ($a' = \mu_{s'}/\mu_{s'} + \mu_a$) and $K = (1+r)/(1-r)$, where r is the internal diffuse reflectance expressed by

$$r = -1.44n_{rel}^{-2} + 0.71n_{rel}^{-1} + 0.668 + 0.0636n_{rel} \tag{8}$$

where n_{rel} is the relative index of refraction (i.e. the ratio of the refractive index of pasteurized milk n_{milk} to the refractive index of air n_{air}), that is, $n_{rel} = n_{milk}/n_{air}$.

It is noteworthy to say that the scattering coefficient can be determined using eq. (6) given that $\mu_a = \mu_t - \mu_s$ where μ_t is the resulting attenuation coefficient from collimated transmission measurements as described above. In addition, the anisotropy factor g in this study is assumed to have a value of 0.95 for the pasteurized milk sample nearly the same anisotropy factor value of biological tissue [16,20].

Then, the collected transmission and diffuse reflectance spectra were analyzed in origin software (Origin Inc. USA) for estimating the optical properties of the samples based on the theoretical formulae mentioned above. Curve fitting was implemented in Origin software as well. To summarize the experimental and theoretical steps taken in this work, Fig. 3 presents the flowchart of the procedure used in this study for the determination of the optical properties of the pasteurized milk samples.

3. Results and discussion

The relationship between the attenuation coefficient of milk and its concentration was experimentally examined for low-fat and full-fat milk samples. Optical measurements concerning collimated transmittance and diffuse reflectance were carried out for all the optical phantom groups used in this work. Fig. 4 shows the detected transmittance and reflectance spectra at 690 nm as a function of volume concentration for low-fat milk phantoms. As expected, the transmittance spectrum decreases with the increased concentration of low-fat milk at 690 nm whereas, the reflectance spectrum increases with the increased concentration of low-fat milk at 690 nm.

Similarly, the transmittance spectra decrease with an increased concentration of low-fat milk at 830 whereas, the reflectance spectra increase with an increased concentration of full-fat milk at 830 nm as shown in Fig. 5a and Fig. 5b respectively. Likewise, the same trends in spectral behavior were found for full fat pasteurized milk samples at 690 and 830 nm.

To evaluate the relationship between transmittance/reflectance spectroscopy and the concentration of milk. Transmittance and reflectance values at 690 nm and 830 nm were extracted from the respected spectra and plotted as a function of concentration as shown in Fig. 6a and Fig. 6b respectively.

Fig. 7(a–d) shows the variation in extinction coefficients at 690 and 830 nm of milk with increased concentration. Extinction coefficients were calculated for both low and full-fat milk samples used in this study as presented in Fig. 7. The output data were fitted linearly according to the fitting equations listed in Table 1 along with the corresponding R-square values for both low and fat milk samples used in this study at 690

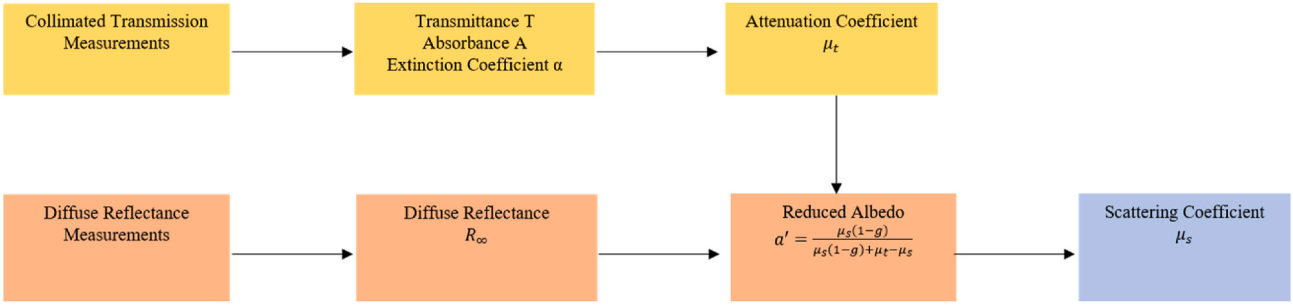

Fig. 3. Flowchart of the procedure for the determination of optical properties of pasteurized milk.

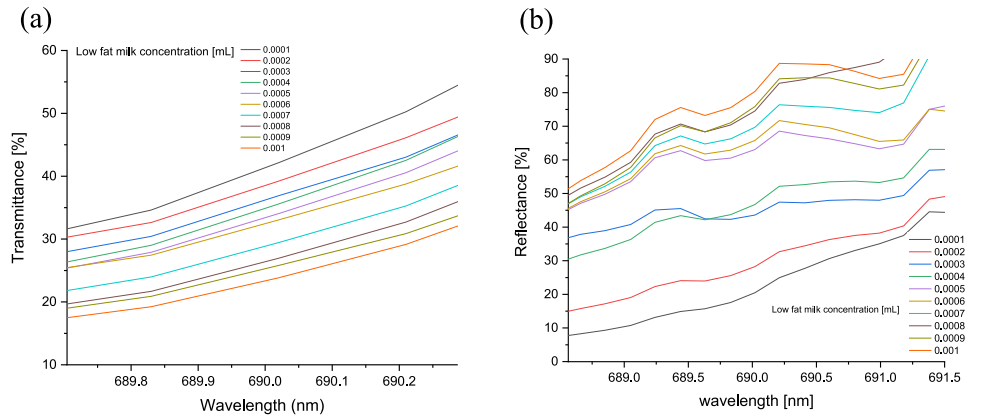

Fig. 4. Transmittance (a) and reflectance spectra (b) of low-fat milk as at 690 nm for different milk concentrations.

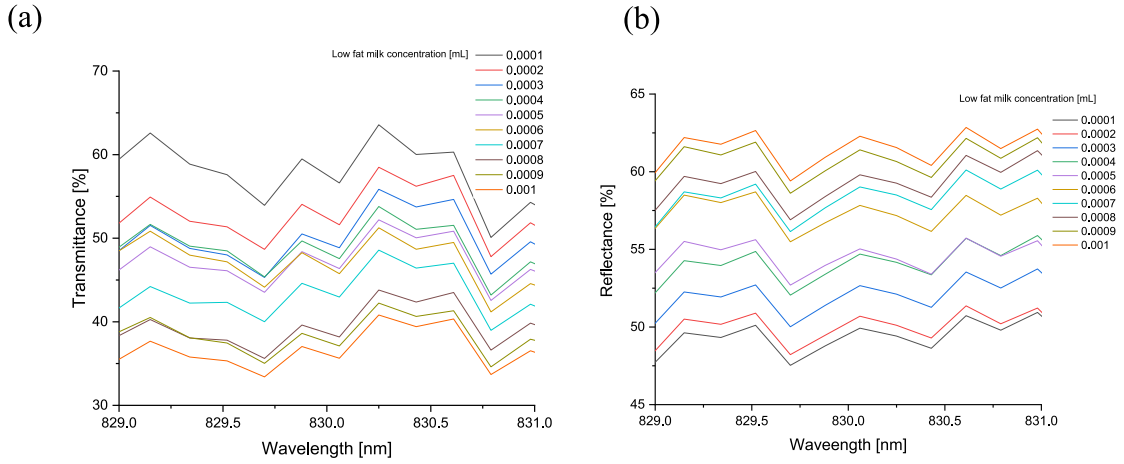

Fig. 5. Transmittance (a) and reflectance spectra (b) of low-fat milk at 830 nm different milk concentrations.

and 830 nm.

From Table .1 it can be said that all fitting results according to R-square values are acceptable.

However, the best fitting was for low-fat pasteurized milk samples at 690 nm and 830 nm in comparison with full-fat pasteurized milk samples. This can be interpreted by increased inhomogeneity in full-fat scattering particles that may result in a weaker correlation between milk concentration and its corresponding scattering coefficient.

As a result, the scattering coefficient of the pasteurized milk can be estimated based on the linear fitting model of the data, and consequently, the scattering coefficient can be set for a given value of concentration.

It is also important to note that the estimated scattering coefficient of the pasteurized milk was found to be nearly equal to the attenuation coefficient of the milk taking into account the negligible value of the absorption coefficient of milk. To validate this assumption, the Absorbance of all milk samples used in this study was calculated based on the Beer-Lambert law mentioned above and found to be less than 1[%] for all samples.

As for scattering, it can be seen from Fig. 8a that the extinction coefficient of low-fat milk samples exhibits higher values at both 690 nm and 830 nm. This can be explained by the higher absorptivity of full-fat

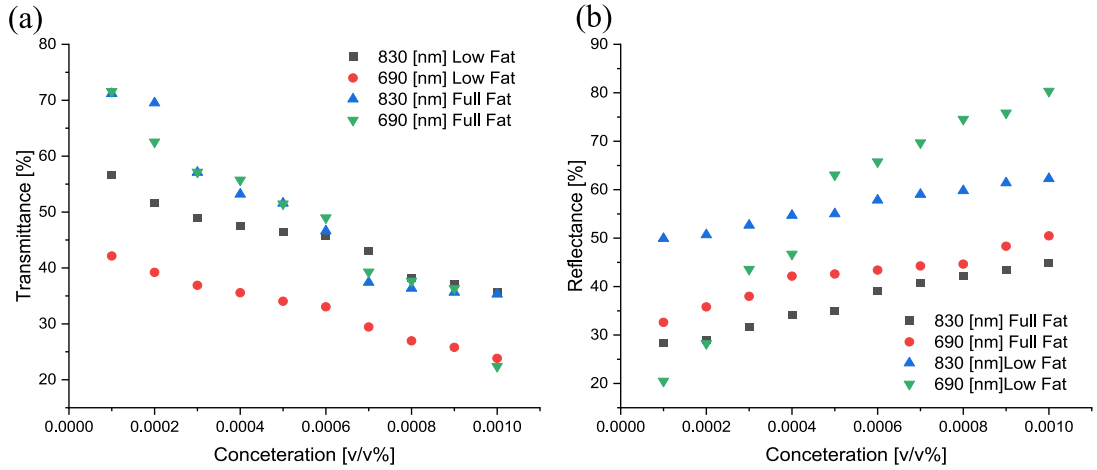

Fig. 6. (a) Transmittance of low and full-fat milk at 690 nm 830 nm (b) reflectance of low and full-fat milk at 690 nm and 830 nm for different milk concentrations.

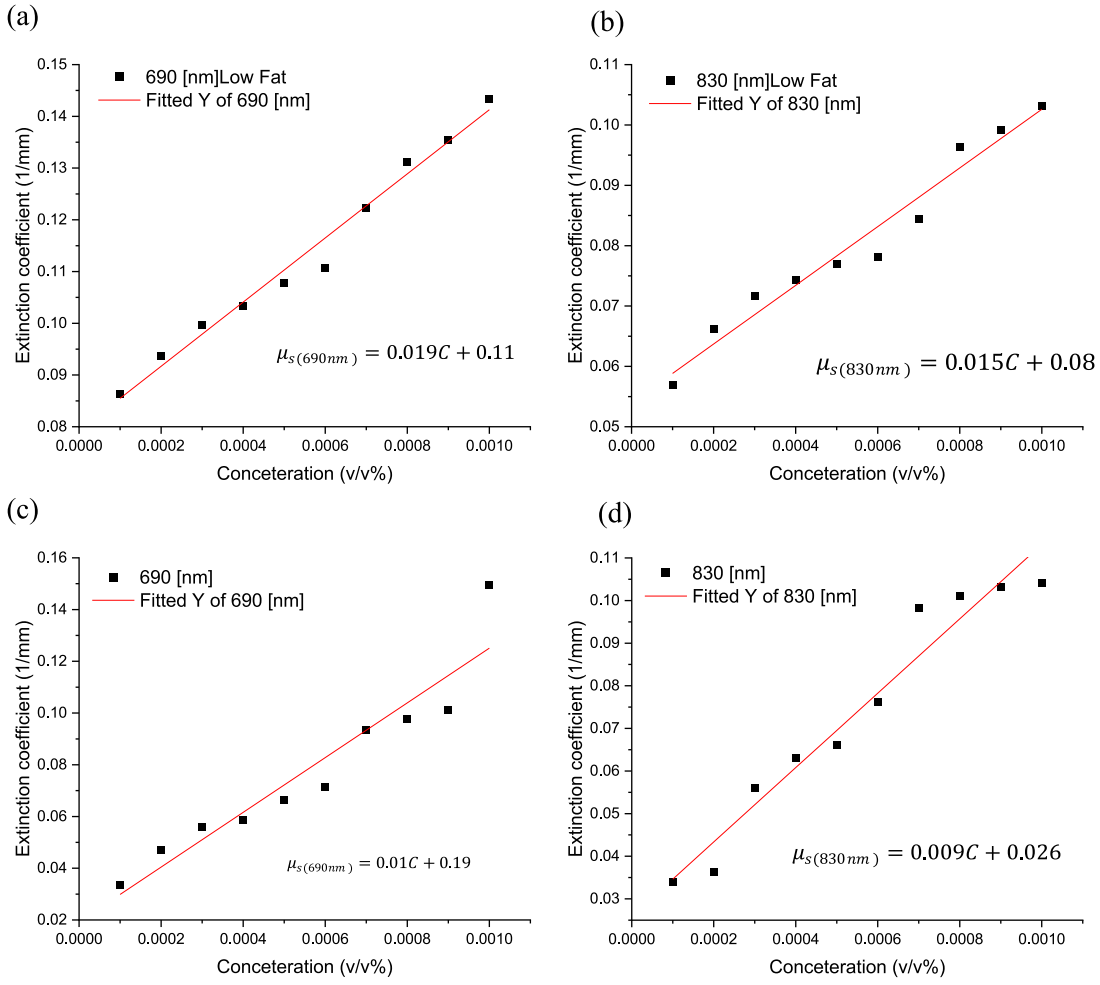

Fig. 7. Fitting curves for the relations between extinction coefficient of pasteurized milk and concentration for low-fat milk samples at (a) 690 nm, (b) for low-fat milk samples at 830 nm, (c) for full-fat milk samples at 690 nm, and (d) for full-fat milk samples at 830 nm.

samples in comparison with low-fat samples.

Additionally, the albedo of the milk samples was also estimated given the values of scattering and absorption coefficients.

Fig. 8b shows the estimated albedo as a function of milk concentration. It can be observed that albedo values for both low and full-fat samples can be as high as 0.9. This indicates that pasteurized milk as a scattering material can be used for optical phantom development that has albedo similar to corresponding values of biological tissue which is nearly around 0.9 on average for most scattering tissues.

One can also notice the low values of albedo for low-fat milk samples,

Table 1
The fitting equations are used for estimating the scattering coefficient of pasteurized milk samples.

Milk type	Wavelength	Fitting Eq.	R^2
Low fat	690 nm	$\mu_{s(690nm)} = 0.019C + 0.11$	0.98
	830 nm	$\mu_{s(830nm)} = 0.015C + 0.08$	0.96
Full fat	690 nm	$\mu_{s(690nm)} = 0.01C + 0.19$	0.90
	830 nm	$\mu_{s(830nm)} = 0.009C + 0.026$	0.95

especially for low concentrations of milk in comparison with other samples. This can be explained by the lower scattering coefficient for low-fat milk due to the larger distance between scattering particles in low-fat milk samples resulting from a low concentration of milk.

The optical methods that we use in this work i.e. NIR laser diffuse reflectance and collimated transmission spectroscopy were used by Shahin and Bachir [21] for optical characterization of intralipid 20%, however, the broadband light source, in the current investigation, was replaced with laser sources that are commonly used for NIR spectroscopic measurements. This demonstrates the applicability of using individual laser sources particularly 830 nm and 690 nm lasers for diffuse reflectance and collimated transmission methods.

Although milk as a scattering constituent has been used previously in building optical phantoms for biophotonic measurements, optical characterization of pasteurized milk and its optical properties have not been investigated. The findings also reveal a difference in optical properties between low-fat and full-fat milk. This is consistent with another work by Cabassi et al. [22] in which the effect of fat on the optical properties of milk was examined.

Furthermore, it is interesting to note that the effect of ultrasonic homogenization on the Vis/NIR bulk optical properties of milk was examined thoroughly by Aernouts et al. [20]. Decreasing the diameter of the fat globules results in reducing the visible (Vis) and near-infrared (NIR) bulk scattering coefficient and scattering anisotropy factor and making them more wavelength dependent.

In another study conducted by Yun and Imm [23], they concluded that based on Fourier Transform Infrared (FTIR) spectra of UHT skim milk stored at 23 °C for three weeks, particle size enlargement was due to protein aggregation and the formation of intermolecular β-sheet structures.

Accordingly, our results in this work demonstrated the suitability of using pasteurized milk for constructing an optical phantom with a given scattering coefficient value. This can be achieved with the help of fitting equations that represent the relation between pasteurized milk concentration and the corresponding scattering coefficient.

Nevertheless, to examine the validity of using these formulae, further experimental work was carried out to validate the methods with a different batch of the produced pasteurized milk. Three different optical phantoms were constructed with three different scattering coefficient values. These values were corresponding to realistic values of optical properties taken from the literature [24] at 690 and 830 nm. Recovered values of optical properties of the built phantoms were estimated based on the above formulae. Surprisingly, comparison between the target scattering coefficient values with the constructed coefficient values resulted in large errors mounting up to 40% as shown in Fig. 9.

Of more interest, full-fat milk samples showed larger uncertainty levels than low-fat milk samples. Likewise, this can be explained by the imperfect linearity between full-fat concentration and extinction coefficient as discussed above. These large errors indicate that batch-to-batch variation seems to have a profound impact on the constructed optical phantom.

This discrepancy due to batch-to-batch variation has been reported in the literature for different diffusive materials used to build optical phantoms. For instance, Di Ninni et al. [25] showed that batch-to-batch variation of the reduced scattering coefficient of Intralipid was found to be about 2%.

However, the intralipid as a highly diffuse medium is often produced with standardized homogeneity and consequently, small batch-to-batch variation can be expected. In contrast, commercial pasteurized milk used in this work lacks homogeneity which resulted in a large batch to batch variation in the scattering coefficient of the pasteurized milk investigated in this work.

As a result, based on the findings presented in this work, it is advisable in practice to use the same batch of milk when constructing the optical phantoms to minimize the uncertainty resulting from batch-to-batch variation. Therefore, the results found in this work can be used as a guiding framework for constructing pasteurized milk-based optical phantom.

Several prior studies reported on the relatively short lifetime of optical phantoms containing milk as a scattering component [1]. Yet, the construction of an optical phantom based on milk is still a matter of interest for researchers in the field of biomedical optics and biophotonics due to its wide availability, safety, and low cost.

The current investigation was limited by the small sample size used for evaluating the variation in batch-to-batch measurements of optical properties. Thus, this work can be extended to accurately determine the errors in the estimated scattering coefficient of pasteurized milk not only with different batches but also due to brand-to-brand variation.

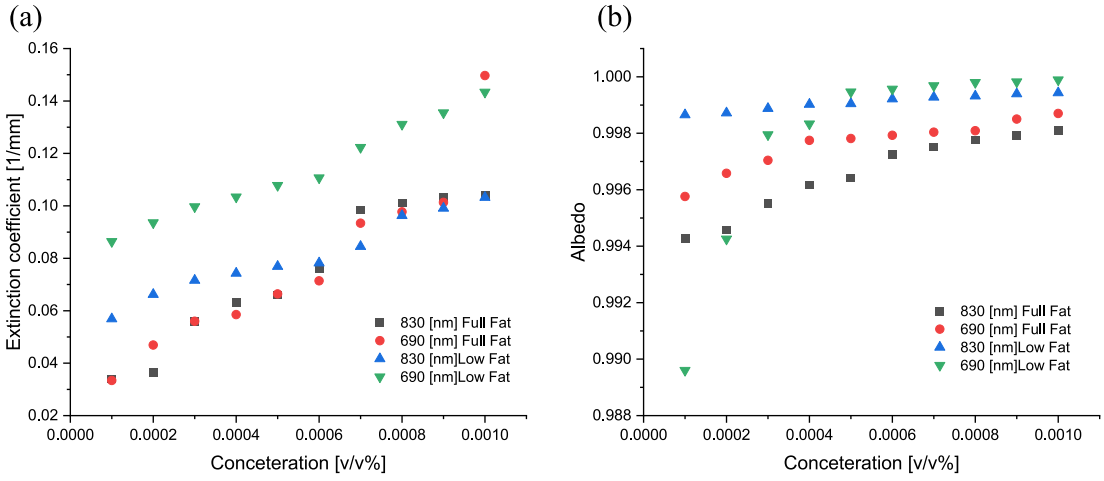

Fig. 8. (a) Extinction coefficient of low and full-fat milk at 690 nm 830 nm as a function of concentration (b) Albedo of low and full-fat milk at 690 nm and 830 nm for different milk concentrations.

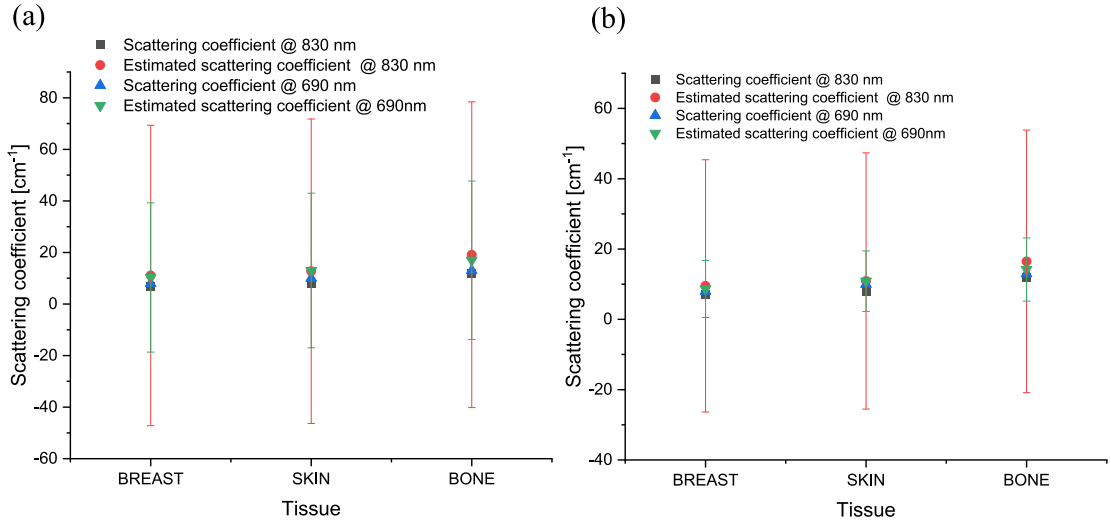

Fig. 9. Uncertainty levels in recovered scattering coefficient of (a) full and (b) low-fat milk at 690 nm 830 nm as a function of concentration and for three different tissue types.

However, this limitation does not impact the significance of the presented findings regarding the utility of pasteurized milk as a potential scattering constituent of optical phantoms.

4. Conclusion

This work was an attempt to investigate the optical properties of pasteurized milk as a scattering material for tissue-like optical phantom construction, particularly in the NIR range of wavelengths. The preliminary results presented above show the suitability of utilizing pasteurized milk for building optical phantoms. However, batch-to-batch variation can result in an erroneous estimation of the scattering coefficient of the constructed optical phantom unless the pasteurized milk is produced in a more controlled manner to minimize inhomogeneity. In addition, Low fat pasteurized milk can be preferably used for mimicking scattering biological tissue at the widely used wavelength of 690 nm and 830 nm in NIR spectroscopy research. Optical parameters estimated using laser transmittance and diffuse reflectance spectroscopy can be viewed as a simple and low-cost guiding approach for developing optical phantoms based on readily available pasteurized milk.

Funding

This work was funded by Damascus University.

CRediT authorship contribution statement

Wesam Bachir: Conceptualization, Methodology, Validation, Writing – review & editing, Supervision. **Rewa khir:** Investigation, Data curation, Writing – original draft, Software, Visualization.

Declaration of competing interest

The authors declare that they have no competing financial interests or personal relationships that influence the work reported in this paper.

References

[1] B.W. Pogue, M.S. Patterson, Review of tissue simulating phantoms for optical spectroscopy, imaging and dosimetry, J. Biomed. Opt. 11 (2006), https://doi.org/10.1117/1.2335429.
[2] A. Mustari, I. Nishidate, M.A. Wares, T. Maeda, S. Kawauchi, S. Sato, M. Sato, Y. Aizu, Agarose-based tissue mimicking optical phantoms for diffuse reflectance spectroscopy, JoVE 2018 (2018), https://doi.org/10.3791/57578.
[3] L. Ntombela, B. Adeleye, N. Chetty, Low-cost fabrication of optical tissue phantoms for use in biomedical imaging, Heliyon 6 (2020), https://doi.org/10.1016/j.heliyon.2020.e03602.
[4] E. Amidi, G. Yang, K.M.S. Uddin, R. Wahidi, Q. Zhu, Low-cost ultrasound and optical gelatin-based phantoms. https://doi.org/10.1117/12.2507938, 2019.
[5] N. Tomm, L. Ahnen, H. Isler, S. Kleiser, T. Karen, D. Ostojic, M. Wolf, F. Scholkmann, Characterization of the optical properties of color pastes for the design of optical phantoms mimicking biological tissue, J. Biophot. 12 (2019), https://doi.org/10.1002/jbio.201800300.
[6] P. Lai, X. Xu, L.V. Wang, Dependence of optical scattering from Intralipid in gelatin-gel based tissue-mimicking phantoms on mixing temperature and time, J. Biomed. Opt. 19 (2014), https://doi.org/10.1117/1.jbo.19.3.035002.
[7] M. Lepore, I. Delfino, Intralipid-based phantoms for the development of new optical diagnostic techniques, open biotechnol, J 13 (2019), https://doi.org/10.2174/1874070701901301 63.
[8] A. Shahin, M.S. El-Daher, W. Bachir, Determination of the optical properties of intralipid 20% over a broadband spectrum, Photonics Lett. Pol 10 (2018), https://doi.org/10.4302/plp.v10i4.843.
[9] S. Stocker, F. Foschum, P. Krauter, F. Bergmann, A. Hohmann, C. Scalfi Happ, A. Kienle, Broadband optical properties of milk, appl, Spectroscopy (Amst.) 71 (2017), https://doi.org/10.1177/0003702816666289.
[10] F. Kamran, P.E. Andersen, Sensitivity analysis for oblique incidence reflectometry using Monte Carlo simulations, Appl. Opt. 54 (2015), https://doi.org/10.1364/ao.54.007099.
[11] O.H.A. Abildgaard, F. Kamran, A.B. Dahl, J.L. Skytte, F.D. Nielsen, C.L. Thomsen, P.E. Andersen, R. Larsen, J.R. Frisvad, Non-invasive assessment of dairy products using spatially resolved diffuse reflectance spectroscopy, Appl. Spectrosc. 69 (2015), https://doi.org/10.1366/14-07529.
[12] O.H.A. Nielsen, A.A. Subash, F.D. Nielsen, A.B. Dahl, J.L. Skytte, S. Andersson-Engels, D. Khoptyar, Spectral characterisation of dairy products using photon time-of-flight spectroscopy, J. Near Infrared Spectrosc. 21 (2013), https://doi.org/10.1255/jnirs.1075.
[13] B. Aernouts, R. Van Beers, R. Watté, T. Huybrechts, J. Lammertyn, W. Saeys, Visible and near-infrared bulk optical properties of raw milk, J. Dairy Sci. 98 (2015), https://doi.org/10.3168/jds.2015-9630.
[14] P. Jain, S.E. Sarma, Light scattering and transmission measurement using digital imaging for online analysis of constituents in milk, Opt. Meas. Syst. Ind. Insp. IX (2015), https://doi.org/10.1117/12.2184903.
[15] R. Michels, F. Foschum, A. Kienle, Optical properties of fat emulsions, Opt Express 16 (2008), https://doi.org/10.1364/oe.16.005907.
[16] J. Gunther, H. Lu, S. Andersson-Engels, Combination of diffuse reflectance and transmittance spectroscopy to obtain optical properties of liquid phantoms, Opt. Eng. 59 (2020), https://doi.org/10.1117/1.oe.59.2.024109.
[17] D.A. Skoog, D.M. West, F.J. Holler, S.R. Crouch, Fundamentals of analytical chemistry, Ninth Editio (2014).
[18] Handbook of Optical Biomedical Diagnostics, Light-tissue interaction. https://doi.org/10.1117/3.2219603, 2017, 1.
[19] S.T. Flock, S.L. Jacques, B.C. Wilson, W.M. Star, M.J.C. van Gemert, Optical properties of intralipid: a phantom medium for light propagation studies, Lasers Surg, Med 12 (1992), https://doi.org/10.1002/lsm.1900120510.
[20] B. Aernouts, R. Van Beers, R. Watté, T. Huybrechts, J. Jordens, D. Vermeulen, T. Van Gerven, J. Lammertyn, W. Saeys, Effect of ultrasonic homogenization on the

Vis/NIR bulk optical properties of milk, Colloids Surf. B Biointerfaces 126 (2015), https://doi.org/10.1016/j.colsurfb.2015.01.004.
[21] A. Shahin, W. Bachir, Broadband spectroscopy for characterization of tissue-like phantom optical properties, Pol. J. Med. Phys. Eng. 23 (2017), https://doi.org/10.1515/pjmpe-2017-0020.
[22] G. Cabassi, M. Profaizer, L. Marinoni, N. Rizzi, T.M.P. Cattaneo, Estimation of fat globule size distribution in milk using an inverse light scattering model in the near infrared region, J. Near Infrared Spectrosc. 21 (2013), https://doi.org/10.1255/jnirs.1070.
[23] S.Y. Yun, J.Y. Imm, Changes in particle size, sedimentation, and protein microstructure of ultra-high-temperature skim milk considering plasmin concentration and storage temperature, Molecules 26 (2021), https://doi.org/10.3390/molecules26082339.
[24] S.L. Jacques, Optic. Properties. Biol. Tissues: A review, Phys. Med. Biol (2013), https://doi.org/10.1088/0031-9155/58/11/R37.
[25] P. Di Ninni, F. Martelli, G. Zaccanti, Intralipid: towards a diffusive reference standard for optical, Phys. Med. Biol. 56 (2011), https://doi.org/10.1088/0031-9155/56/2/N01.